A NUMERICAL SCHEME FOR DARCY-FORCHHEIMER FLOW OF NON-NEWTONIAN NANOFLUID UNDER THE EFFECTS OF CONVECTIVE AND ZERO MASS FLUX BOUNDARY CONDITIONS

by

Muhammad Shoaib ARIF[a,b*], Wasfi SHATANAWI[a,c,d], and Yasir NAWAZ[b]

[a] Department of Mathematics and Sciences, College of Humanities and Sciences, Prince Sultan University, Riyadh, Saudi Arabia
[b] Department of Mathematics, Air University, PAF Complex E-9, Islamabad, Pakistan
[c] Department of Medical Research, China Medical University, Taichung, Taiwan
[d] Department of Mathematics, Faculty of Science, The Hashemite University, Zarqa, Jordan

Original scientific paper
https://doi.org/10.2298/TSCI221230076A

This research aims to propose a numerical scheme for solving boundary value problems. It is a two-stage, third-order accurate scheme known as a predictor-corrector scheme. The two main results are finding the region of the scheme where it is stable and determining the stability criterion for a set of linearized first-order differential equations. In addition, a mathematical model for heat and mass transfer of Darcy-Forchheimer flow of non-Newtonian nanofluid over the sheet is presented. The similarity transformations reduce PDE into a system of ODE for easier manipulation. The results are compared with the past research and those obtained by MATLAB SOLVER BVP4C. The results show that the velocity profile slightly decays by enhancing the Weisenberg number.

Key words: *proposed numerical scheme, stability, non-Newtonian fluid, Darcy-Forchheimer flow, shooting method*

Introduction

There are several applications of non-Newtonian liquids which serve as mechanical processes in engineering industries. Categories of non-Newtonian fluid into shear thickening and shear thinning impart variations during heat transport operations. Therefore, one can focus on the heat transport attribute of non-Newtonian fluids to enhance the thermal conducting efficiency of such fluids. A detailed understanding of the fundamentals of physical principles and rheological properties governing fluid-flow provides insight into the limitations and delimitations of liquid flow. Such processes are often described as modelling with a strong theoretical background. Mathematical modelling has shown that a reduction in the experimental data needed to evaluate the effect of process variables can be achieved by achieving an agreement between theory and experiment for the free-draining flow. In Peralta *et al.* [1], researchers set out to develop a mathematical model for the free-draining flow during the draining stage of a dip-coating process on a finite vertical plate using the Carreau-Yasuda model fluid and then locate analytical solutions for the corresponding fluid-dynamic variables.

* Corresponding author, e-mail: marif@psu.edu.sa, wshatanawi@psu.edu.sa

Khan *et al.* [2] examines the dynamical behavior of a binary mixture embedded in a porous material as it moves through a thermal radiation field and a non-Newtonian fluid with heat source/sink features. Non-Newtonian viscoelastic fluid turbine disk cooling is analyzed using the homotopy analysis method [3]. In Mahmood *et al.* [4], the Carreau Yasuda fluid model is tested in a lid-driven cavity and channel with an obstruction, with kinetic energy measurements and drag and lift coefficients.

In Khan *et al.* [5], the Carreau-Yasuda fluid-flow is represented using an energy equation considering the Soret and Dufour effects on a porous surface. The Lattice Boltzmann method models thermo-solutal natural convection and entropy production in a cubic cavity filled with a non-Newtonian Carreau-Yasuda fluid [6]. Over a deformable sheet, in Khan *et al.* [7], consider the incompressible flow of a non-Newtonian fluid (Carreau-Yasuda fluid). The concept of a porous media is examined. Activation energy is taken into account for chemical reactions that take place on a sheet's surface.

Several industrial situations, like removing wastes from tubes, reservoirs, or tanks and a stage of batch dip-coating, observe a physical phenomenon named free-draining flow [8-11]. Fluid drainage can thin a surface by covering whatever it drains off. This is crucial for regulating the final film quality using a dip-coating technique [8, 12].

For this reason, theoretical analysis can be a cost-effective means of evaluating potential coating options [13]. Analytical solutions are currently viewed as a viable option for solving mathematical problems due to their desirable characteristics [14].

Eley *et al.* [15] suggested that it is arduous to use a mathematical expression to prove a connection between the transport phenomenon and the rheological behavior of governing fluid during the coating process. A huge effort has been made to find a new analytical solution for solving mathematical models that can narrate fluid thermal convection factors like velocity and film thickness profiles. Incorporating these elements into an expression, an equation accurately represents the rheological behavior of an unusual fluid throughout the dip-coating process drainage phase.

A profound work is done by [16, 17] to reckon the steady state viscosity of a non-Newtonian fluid through a well-known model named The Carreau-Yasuda model [18] suggested a continuum mechanics foundation for this contrary. It is an empirical rheological model. Fluids are described as a dispersion of particles in which Brownian and hydrodynamic forces are the principal interacting forces [19, 20] and can be classified as either a dispersed or continuous phase material [21].

Hall and Ohmic effects in an asymmetric channel on the Carreau-Yasuda model were investigated by [22]. Flow behavior of the Carreau-Yasuda model with Hall effects subject to curved channel was observed by [23], whereas [24] examined the flow of Carreau-Yasuda fluid with the free draining flow on a vertical plate. In Rehman *et al.* [25], the authors examine the effect of Soret and Dufour on electroosmotic forces in the flow of Casson fluid towards a stretchy sheet. For a family of non-linear impulsive nabla fractional difference equations of order alpha, we prove sufficient criteria on the existence and uniqueness of solutions in [26]. For the second-order iterative dynamic boundary value problem with mixed derivative operators, the authors of [27] construct adequate conditions for the existence and uniqueness of solutions.

Various numerical methods have been proposed to study boundary-layer flows in the literature. Sometimes, with the help of suitable transformations, the governing equations of boundary layer flows can be written as an ODE or system of ODE. This system of ODE is required to solve by some analytical or numerical scheme. Various authors have employed

shooting methods based on Runge-Kutta methods from these discussed cases of boundary-layer flows. This contribution proposes a numerical scheme for solving linear and non-linear scalar and system ODE. The scheme is employed for solving the system of boundary value problems. This system is obtained by transforming the system of equations governing heat and mass transfer of non-Newtonian nanofluid-flow over a moving sheet.

Proposed numerical scheme

This article discusses a numerical technique for resolving ODE. The scheme is two-stage. The first stage of the scheme is an extended form of the classical forward Euler scheme using Taylor series expansion. The first stage of the scheme finds the solution at i^{th} grid point and uses the information of the given differential equation at the $(i-1)^{\text{th}}$ grid point. But the solution at this i^{th} grid point is updated in the next stage. The first stage of the scheme is just a predictor stage, and the corrector stage is the second stage. So in the second stage, the solution of the given differential equation is calculated with some particular accuracy. To begin the numerical scheme construction procedure, consider the following differential equation:

$$y' = f(y) \tag{1}$$

subject to the initial condition:

$$y = \alpha_1 \tag{2}$$

where α_1 is constant

For solving eq. (1), the first stage of the scheme can be expressed:

$$\bar{y}_i = y_{i-1} + hy'_{i-1} + h^2 y''_{i-1} \tag{3}$$

where $'$ shows a derivative with respect to the independent variable. The h shows the step size. This stage requires the computation of the second derivative dependent variable. The second stage, or the corrector stage of the scheme, is expressed:

$$y_i = y_{i-1} + h(ay'_i + by'_{i-1} + c\bar{y}'_i) \tag{4}$$

where *a, b,* and *c* are unknown to be determined by employing Taylor series expansion to eq. (4). For doing so, consider a Taylor series expansion for y_{i-1} and y'_{i-1}:

$$y_{i-1} = y_i + hy'_i + \frac{h^2}{2}y''_i + \frac{h^3}{6}y'''_i + O(h^4) \tag{5}$$

$$y'_{i-1} = y'_i + hy''_i + \frac{h^2}{2}y'''_i + O(h^3) \tag{6}$$

Substituting eqs. (3), (5), and (6) into eq. (4), yields:

$$y_i = y_i - hy'_i + \frac{h^2}{2}y''_i - \frac{h^3}{6}y'''_i + h\left(ay'_i + by'_i - bhy''_i + \frac{bh^2}{2}y'''_i + cy'_i + \frac{ch^2}{2}y'''_i\right) \tag{7}$$

Equating coefficients of $hy'_i, h^2y''_i$, and $h^3y'''_i$ on both sides of eq. (7), it gives:

$$0 = -1 + a + b + c \tag{8}$$

$$0 = \frac{1}{2} - b \tag{9}$$

$$0 = \frac{1}{6} + \frac{c}{2} \tag{10}$$

By solving eqs. (8)-(10), yields:

$$a = \frac{2}{3}, \quad b = \frac{1}{2}, \quad c = \frac{1}{6} \tag{11}$$

Thus the corrector stage of the proposed scheme for solving eq. (1) is:

$$y_i = y_{i-1} + h\left(\frac{2}{3}y_i' + \frac{1}{2}y_{i-1}'' - \frac{1}{6}\overline{y}_i'\right) \tag{12}$$

By looking at eq. (1), predictor and corrector stages, respectively, are:

$$\overline{y}_i = y_{i-1} + hf_i + h^2 f_i' \tag{13}$$

$$y_i = y_{i-1} + h\left(\frac{2}{3}f_i + \frac{1}{2}f_{i-1} - \frac{1}{6}\overline{f}_i\right) \tag{14}$$

where $f_i = f(y_i)$ and f'_i is derivative of f with respect to independent variables.

Scalar stability

We can determine where the proposed scheme for eq. (1) is most stable using linearization. The linearized equation is:

$$y' = \lambda y \tag{15}$$

After implementing the first step of the suggested scheme, from eq. (15) we get:

$$\overline{y}_i = y_{i-1} + h\lambda y_{i-1} + h^2\lambda^2 y_{i-1} = (1 + h\lambda + h^2\lambda^2)y_{i-1} \tag{16}$$

Employing the second stage of the proposed scheme to eq. (15), which yields:

$$y_i = y_{i-1} + h\left(\frac{2}{3}\lambda y_i + \frac{1}{2}\lambda y_{i-1} - \frac{1}{6}\lambda\overline{y}_i\right) \tag{17}$$

Substituting eq. (16) into eq. (17) and letting $z = \lambda h$ leads to:

$$y_i = y_{i-1} + \left[\frac{2}{3}zy_i + \frac{1}{2}zy_{i-1} - \frac{1}{6}z(1 + z + z^2)\right] \tag{18}$$

Re-write eq. (18) as:

$$y_i = \frac{1 + \frac{1}{2}z - \frac{1}{6}z(1 + z + z^2)y_{i-1}}{1 - \frac{2}{3}z} \tag{19}$$

The stability condition is expressed:

$$\left|\frac{1+\frac{1}{2}z-\frac{1}{6}z(1+z+z^2)}{1-\frac{2}{3}z}\right|<1 \tag{20}$$

where $z = \lambda h$.

Stability for the matrix-vector equation

The goal is to determine whether or not a set of linear first-order differential equations is stable. Consider the following matrix-vector equation:

$$\vec{\mathrm{u}}' = \mathrm{A}\vec{\mathrm{u}} \tag{21}$$

where $\vec{\mathrm{u}}$ is a vector of order 3 × 1 and A – a matrix of order 3 × 3. Before finding the stability condition, a proposed scheme will be applied to solve eq. (21), so employing the first stage of the proposed scheme and using the Gauss-Seidel iterative method on eq. (21) it yields:

$$\vec{\mathrm{u}}_i^{k+1} = \vec{\mathrm{u}}_{i-1}^{k+1} + h\mathrm{A}\vec{\mathrm{u}}_{i-1}^{k+1} + h^2\mathrm{A}^2\vec{\mathrm{u}}_{i-1}^{k+1} \tag{22}$$

Applying the second stage, or corrector stage on eq. (21), is obtained:

$$\vec{\mathrm{u}}_i^{k+1} = \vec{\mathrm{u}}_{i-1}^{k+1} + h\left(\frac{2}{3}\mathrm{A}\vec{\mathrm{u}}_i^{k} + \frac{1}{2}\mathrm{A}\vec{\mathrm{u}}_{i-1}^{k+1} - \frac{1}{6}\mathrm{A}\bar{\vec{\mathrm{u}}}_i^{k+1}\right) \tag{23}$$

In the initial procedure of stability analysis following transformation is considered:

$$\begin{aligned} \bar{\vec{\mathrm{u}}}_i^{k+1} &= \bar{\vec{\mathrm{E}}}^{k+1}e^{iI\psi}, \quad \vec{\mathrm{u}}_{i-1}^{k+1} = \vec{\mathrm{E}}^{k+1}e^{(i-1)I\psi} \\ \vec{\mathrm{u}}_i^{k+1} &= \vec{\mathrm{E}}^{k+1}e^{iI\psi}, \quad \vec{\mathrm{u}}_i^{k} = \vec{\mathrm{E}}^{k}e^{iI\psi} \end{aligned} \tag{24}$$

where $I = \sqrt{-1}$.

Substituting some of the transformations from eq. (24) into eq. (22) yields:

$$\bar{\vec{\mathrm{E}}}^{k+1}e^{iI\psi} = \vec{\mathrm{E}}^{k+1}e^{iI\psi} + h\mathrm{A}\vec{\mathrm{E}}^{k+1}e^{(i-1)I\psi} + h^2\mathrm{A}^2\vec{\mathrm{E}}^{k+1}e^{(i-1)I\psi} \tag{25}$$

Dividing both sides of eq. (25) by $e^{iI\psi}$ and resulting equation becomes:

$$\vec{\mathrm{E}}^{k+1} = e^{-I\psi}\vec{\mathrm{E}}^{k+1} + h\mathrm{A}\vec{\mathrm{E}}^{k+1}e^{-I\psi} + h^2\mathrm{A}^2\vec{\mathrm{E}}^{k+1}e^{-I\psi} \tag{26}$$

Substitute the relevant transformation from eq. (24) into eq. (23) and divide both sides of the equation by $e^{iI\psi}$, obtains:

$$\vec{\mathrm{E}}^{k+1} = e^{-I\psi}\vec{\mathrm{E}}^{k+1} + h\left(\frac{2}{3}\mathrm{A}\vec{\mathrm{E}}^{k} + \frac{1}{2}\mathrm{A}\vec{\mathrm{E}}^{k+1}e^{-I\psi} - \frac{1}{6}\mathrm{A}\vec{\mathrm{E}}^{k+1}\right) \tag{27}$$

Using eq. (26) in eq. (27) gives:

$$\vec{\mathrm{E}}^{k+1} = e^{-I\psi}\vec{\mathrm{E}}^{k+1} + h\left(\frac{2}{3}\mathrm{A}\vec{\mathrm{E}}^{k} + \frac{1}{2}\mathrm{A}\vec{\mathrm{E}}^{k+1}e^{-I\psi} - \frac{1}{6}\mathrm{A}\mathrm{A}_1\vec{\mathrm{E}}^{k+1}e^{-I\psi}\right) \tag{28}$$

where $A_1 = I \cdot D + hA + h^2A^2$, and ID is an identity matrix of order 3 × 3.

$$\left(I\cdot D - e^{-I\psi} I\cdot D - \frac{1}{2}hAe^{-I\psi} + \frac{h}{6}AA_1e^{-I\psi}\right)\vec{E}^{k+1} = \frac{2}{3}hA\vec{E}^{k} \tag{29}$$

The stability conditions can be expressed:

$$\left|\frac{\frac{2}{3}h\lambda_A}{1 - e^{-I\psi} - \frac{1}{2}h\lambda_A e^{-I\psi} + \frac{h}{6}\lambda_{AA_1}e^{-I\psi}}\right| < 1 \tag{30}$$

where λ_A and λ_{AA_1} are respectively eigenvalues of A and AA_1.

Problem formulation

Consider the steady laminar, 2-D, and incompressible Carreau Yasuda nanofluid-flow over the moving sheet. Let u and v be a horizontal and vertical component of the velocity. The x-axis is taken along the plate, and y-axis is perpendicular to x-axis. The flow is generated by the sudden movement of the plate along the positive x-axis. Let the moving velocity be presented by u_w. Let T and C be the temperature of the fluid and concentration, respectively. The T_w and C_w are temperature and concentration at the wall and T_∞ and C_∞ denotes the temperature and concentration away from the plate. We have a conducting, magnetic fluid if the fluid conducts electricity and the magnetic field is supplied perpendicular to the motion.

Consider the Darcy Forchheimer characteristic, and under the assumption of boundary layer theory and following [28], the equations that describe flow phenomena are:

$$\frac{\partial u}{\partial x} + \frac{\partial v}{\partial y} = 0 \tag{31}$$

$$u\frac{\partial u}{\partial x} + v\frac{\partial v}{\partial y} = v\frac{\partial^2 v}{\partial y^2} + \Gamma^d v\left(\frac{n-1}{d}\right)(d+1)\frac{\partial^2 u}{\partial y^2}\left(\frac{\partial u}{\partial y}\right)^d - \frac{\sigma}{\rho}B_o^2 u - \frac{v}{k_p}u - Fu^2 \tag{32}$$

$$u\frac{\partial T}{\partial x} + v\frac{\partial T}{\partial y} = \alpha\frac{\partial^2 T}{\partial y^2} + \frac{\mu}{\rho c_p}\left(\frac{\partial u}{\partial y}\right)^2 \frac{\mu}{\rho c_p}\Gamma^d\left(\frac{n-1}{d}\right)\left(\frac{\partial u}{\partial y}\right)^2\left(\frac{\partial u}{\partial y}\right)^d + \\ + \tau\left[D_B\frac{\partial C}{\partial y}\frac{\partial T}{\partial y} + \frac{D_T}{T_\infty}\left(\frac{\partial T}{\partial y}\right)^2\right] - \frac{1}{\rho c_p}\frac{\partial q_r}{\partial y} \tag{33}$$

$$u\frac{\partial C}{\partial x} + v\frac{\partial C}{\partial y} = D_B\frac{\partial^2 C}{\partial y^2} + \frac{D_T}{T_\infty}\frac{\partial^2 T}{\partial y^2} - k_1(C - C_\infty) \tag{34}$$

subject to the boundary conditions:

$$\begin{aligned} u = U_w, \quad v = 0, \quad T = T_w, \quad C = C_w, \quad \text{when } y = 0 \\ u \to 0, \quad T \to T_\infty, \quad C \to C_\infty, \quad \text{when } y \to \infty \end{aligned} \tag{35}$$

To reduce eqs. (31)-(35) into the dimensionless system of equations, the following transformations are considered:

$$\eta = \sqrt{\frac{a}{v}}y, \quad u = axf', \quad v = -\sqrt{av}f, \quad \theta = \frac{T - T_\infty}{T_\mathrm{w} - T_\infty}, \quad \phi = \frac{C - C_\infty}{C_\mathrm{w} - C_\infty} \tag{36}$$

Under transformation (36), eqs. (32)-(35) are reduced to:

$$f'^2 - ff'' = f''' + \frac{n-1}{d}(d+1)(W_e)^d f'''f''^d - Mf' - \beta f'' - F_r f'^2 \tag{37}$$

$$f\theta' + \frac{1}{P_r}\left(1 + \frac{4}{3}R_d\right)\theta'' + E_c f''^2 + \frac{n-1}{d}E_c(W_e)^d f''^2 f''^d + N_b\theta'\phi' + N_t\theta'^2 = 0 \tag{38}$$

$$-f\phi' = \frac{1}{S_c}\phi'' + \frac{N_t}{N_b}\theta'' - \gamma\phi \tag{39}$$

subject to the dimensionless boundary conditions:

$$\begin{gathered} f = 0, \quad f' = 1, \quad \theta' = -B_1(1-\theta), \quad N_t\theta' + N_b\phi' = 0, \quad \text{when } \eta = 0 \\ f' \to 0, \quad \theta \to 0, \quad \phi \to 0, \quad \text{when } \eta \to \infty \end{gathered} \tag{40}$$

A system of the first-order differential equation is established for solving eqs. (37)-(40) using the proposed scheme. To do so, consider the following system of fist order differential equations of the form:

$$f' = f_1, \quad f(0) = 0 \tag{41}$$

$$f_1' = f_2, \quad f_1(0) = x_1 \tag{42}$$

$$f_2' = \frac{1}{1 + \frac{n-1}{d}(d+1)(W_e)^d f_2^d}(f_1^2 - ff_2 + Mf_1 + \lambda f_1 + F_r f_1^2), \quad f_2(0) = x_2 \tag{43}$$

$$\theta_1' = \frac{P_r}{1 + \frac{4}{3}R_d}\left[-f\theta_1 - E_c f_2^2 - \frac{n-1}{d}E_c(W_e)^d f_2^2 f_2^d - N_b\theta_1\phi_1 - N_t\theta_1^2\right], \quad \theta_1(0) = x_3 \tag{44}$$

$$\phi' = \phi_1, \quad \phi(0) = x_4 \tag{45}$$

$$\phi_1' = S_c\left\{-f\phi_1 - \frac{N_t}{N_b}\left(\frac{P_r}{1 + \frac{4}{3}R_d}\right)\left[-f\theta_1 - E_c f_2^2 - \frac{n-1}{d}E_c(W_e)^d f_2^2 f_2^d - \right.\right.$$

$$\left.\left. - N_b\theta\phi_1 - N_t\theta_1^2\right] + r\phi\right\}, \quad \phi_1(0) = x_5 \tag{46}$$

For applying a proposed numerical scheme for solving eqs. (41)-(46). To do so, applying the predictor stage to eqs. (41)-(46) that yields:

$$\overline{f_i} = f_{i-1} + hf_{1,i-1} + h^2 f_{2,i-1} \tag{47}$$

$$\overline{f}_{1,i} = f_{1,i-1} + hf_{2,i-1} + \frac{h^2}{1+\frac{n-1}{d}(d+1)(W_e)^d f_{2,i-1}^d} \cdot$$

$$\cdot(f_{1,i-1}^2 - f_{i-1}f_{2,i-1} + Mf_{1,i-1} + \lambda f_{1,i-1} + F_r f_{1,i-1}^2) \tag{48}$$

$$\overline{f}_{2,i} = f_{2,i-1} + \frac{h}{1+\frac{n-1}{d}(d+1)(W_e)^d f_{2,i-1}^d}[f_{1,i-1}^2 - f_{i-1}f_{2,i-1} + (M+\lambda)f_{1,i-1} + F_r f_{1,i-1}^2] -$$

$$-\frac{h^2\frac{n-1}{d}(d+1)(W_e)^d}{\left[1+\frac{n-1}{d}(d+1)(W_e)^d f_{2,i-1}^d\right](3+d)}[f_{1,i-1}^2 - f_{i-1}f_{2,i-1} + (M+\lambda)f_{1,i-1} + F_r f_{1,i-1}^2)^d \cdot$$

$$\cdot[f_{1,i-1}^2 - f_{i-1}f_{2,i-1} + (M+\lambda)f_{1,i-1} + F_r f_{1,i-1}^2] + \frac{h^2}{1+\frac{n-1}{d}(d+1)(W_e)^d f_2^d} \cdot$$

$$\cdot\{f_1 f_2 - \frac{f_{i-1}}{1+\frac{n-1}{d}(d+1)(W_e)^d f_{2,i-1}^d}[f_{1,i-1}^2 - f_{i-1}f_{2,i-1} + (M+\lambda)f_{1,i-1} + F_r f_{1,i-1}^2] +$$

$$+(M+\lambda)f_{2.i-1} + 2F_r f_{1,i-1}f_{2,i-1}\} \tag{49}$$

$$\overline{\theta}_i = \theta_{i-1} + h\theta_{1,i-1} + \frac{h^2 P_r}{1+\frac{4}{3}R_d}\left[-f_{i-1}\theta_{i-1} - E_c f_{2,i-1}^2 - \frac{n-1}{d}E_c(W_e)^d f_{2,i-1}^{2+d} -\right.$$

$$\left. - N_b\theta_{1,i-1}\phi_{1,i-1} - N_t\theta_{1,i-1}^2\right] \tag{50}$$

$$\overline{\theta}_{1,i} = \theta_{1,i-1} + \frac{hP_r}{1+\frac{4}{3}R_d}\left[-f_{i-1}\theta_{i-1} - E_c f_{2,i-1}^2 - \frac{n-1}{d}E_c(W_e)^d f_{2,i-1}^{2+d} - N_b\theta_{1,i-1}\phi_{1,i-1} - N_t\theta_{1,i-1}^2\right] -$$

$$-\frac{h^2 P_r}{1+\frac{4}{3}R_d}\left\{-f_{1,i-1}\theta_{1,i-1} - (f_{i-1} + N_b\phi_{1,i-1} - 2N_t\theta_{1,i-1} - N_t S_c\theta_{i,i-1})\frac{P_r}{1+\frac{4}{3}R_d}\cdot\right.$$

$$\cdot\left[-f_{i-1}\theta_{1,i-1} - E_c f_{2,i-1}^2 - \frac{n-1}{d}E_c(W_e)^d f_{2,i-1}^{2+d} - N_b\theta_{1,i-1}\phi_{1,i-1} - N_t\theta_{1,i-1}^2\right] -$$

$$-\frac{\left[2E_c f_{2,i-1} + \frac{n-1}{d}E_c(W_e)^d(2+d)f_2^{1+d}\right]}{1+\frac{n-1}{d}(d+1)(W_e)^d f_{2,i-1}^d}\left[f_{1,i-1}^2 - f_{i-1}f_{2,i-1} + (M+\lambda)f_{1,i-1} + F_r f_{1,i-1}^2\right] +$$

$$\left. + N_b S_c\theta_{1,i-1}f_{i-1}\phi_{1,i-1} - \gamma N_b S_c\theta_{1,i-1}\phi_{i-1}\right\} \tag{51}$$

$$\bar{\phi}_i = \phi_{i-1} + h\phi_{1,i-1} + h^2 S_c \left\{ -f_{i-1}\phi_{1,i-1} - \left(\frac{N_t}{N_b}\right)\frac{P_r}{1+\frac{4}{3}R - d} \cdot \right.$$

$$\left. \cdot\left[-f_{i-1}\theta_{1,i-1} - E_c f_{2,i-1}^2 - \frac{n-1}{d}E_c (W_e)^d f_{2,i-1}^{2+d} - N_b\theta_{1,i-1}\phi_{1,i-1} - N_t\theta_{1,i-1}^2\right] + \gamma\phi_{i-1}\right\} \tag{52}$$

$$\bar{\phi}_{1,i} = \phi_{1,i-1} + hS_c \left\{ -f_{i-1}\phi_{i-1} - \frac{N_t P_r}{N_b\left(1+\frac{4}{3}R_d\right)}\left[-f_{i-1}\theta_{1,i-1} - E_c f_{2,i-1}^2 - \frac{n-1}{d}E_c (W_e)^d f_{2,i-1}^{2+d} - \right.\right.$$

$$\left.\left. -N_b\theta_{1,i-1}\phi_{1,i-1} - N_t\theta_{1,i-1}^2\right] + \gamma\phi_{i-1}\right\} + h^2 S_c \left\{ -f_{1,i-1}\phi_{1,i-1} - S_c f_{i-1}^2\phi_{1,i-1} + \right.$$

$$+\left[S_c\frac{N_t}{N_b}f_{i-1} + \frac{N_t P_r f_{i-1}}{N_b\left(1+\frac{4}{3}R_d\right)} + \frac{N_t P_r\phi_{1,i-1}}{N_b^2\left(1+\frac{4}{3}R_d\right)} - \frac{N_t^2 P_r S_c\theta_{1,i-1}}{N_b\left(1+\frac{4}{3}R_d\right)} + \frac{2N_t^2 P_r\theta_{1,i-1}}{N_b\left(1+\frac{4}{3}R_d\right)}\right] \cdot$$

$$\cdot\left(\frac{P_r}{1+\frac{4}{3}R_d}\right)\left[-f_{i-1}\theta_{1,i-1} - E_c f_{2,i-1}^2 - \frac{n-1}{d}E_c (W_e)^d f_{2,i-1}^{2+d} - N_b\theta_{1,i-1}\phi_{1,i-1} - N_t\theta_{1,i-1}^2\right] -$$

$$-\gamma S_c f_{i-1}\phi_{i-1} + \frac{N_t P_r f_{1,i-1}\theta_{1,i-1}}{N_b\left(1+\frac{4}{3}R_d\right)} - \left[\frac{N_t P_r\, 2E_{cf\,2,i-1}}{N_b\left(1+\frac{4}{3}R_d\right)} - \frac{(n-1)E_c N_t P_r (W_e)^d (2+d) f_{2,i-1}^{1+d}}{dN_b\left(1+\frac{4}{3}R_d\right)}\right] \cdot$$

$$\cdot\left[\frac{1}{1+\frac{n-1}{d}(d+1)(W_e)^d f_{2,i-1}^d}\right]\left[f_{1,i-1}^2 - f_{i-1}f_{2,i-1} + (M+\lambda)f_{1,i-1} + F_r f_{1,i-1}^2\right] -$$

$$\left. -\frac{N_t P_r S_c\theta_{1,i-1}f_{i-1}\phi_{1,i-1}}{\left(1+\frac{4}{3}R_d\right)} + \frac{rN_t P_r S_c\theta_{1,i-1}\phi_{i-1}}{\left(1+\frac{4}{3}R_d\right)} + \gamma\phi_{1i-1}\right\} \tag{53}$$

Applying the second or corrector stage of the proposed scheme on eqs. (41)-(47), it is obtained

$$f_i = f_{i-1} + h\left(\frac{2}{3}f_{1,i} + \frac{1}{2}f_{1,i-1} - \frac{1}{6}\bar{f}_{1,i}\right) \tag{54}$$

$$f_{1,i} = f_{1,i-1} + h\left(\frac{2}{3}f_{1,i} + \frac{1}{2}f_{1,i-1} - \frac{1}{6}\bar{f}_{1,i}\right) \tag{55}$$

$$f_{2,i} = f_{2,i-1} + \frac{h}{1+\frac{n-1}{d}(d+1)(W_e)^d f_{2,i-1}^d}\left\{\frac{2}{3}\left[f_{1,i}^2 - f_i f_{2,i} + (M+\lambda)f_{1,i} + F_r f_{1,i}^2\right] + \right.$$

$$\left. +\frac{1}{2}\left[f_{1,i-1}^2 - f_{i-1}f_{2,i-1} + (M+\lambda)f_{1,i-1} + F_r f_{1,i-1}^2\right] - \frac{1}{6}\left[\bar{f}_{1,i}^2 - \bar{f}_i\bar{f}_{2,i} + (M+\lambda)\bar{f}_{1,i} + F_r\bar{f}_{1,i}^2\right]\right\} \tag{56}$$

$$\theta_i = \theta_{i-1} + h\left(\frac{2}{3}\theta_{1,i} + \frac{1}{2}\theta_{1,i-1} - \frac{1}{6}\overline{\theta}_{1,i}\right) \tag{57}$$

$$\theta_{1,i} = \theta_{1,i-1} + \frac{hP_r}{1+\frac{4}{3}R_d}\left\{\frac{2}{3}\left[-f_i\theta_i - E_c f_{2,i}^2 - \frac{n-1}{d}E_c(W_e)^d f_{2,i}^{2+d} - N_b\theta_{1,i}\phi_{1,i} - N_t\theta_{1,i}^2\right] + \right.$$
$$+\frac{1}{2}\left[-f_{i-1}\theta_{i-1} - E_c f_{2,i-1}^2 - \frac{n-1}{d}E_c(W_e)^d f_{2,i-1}^{2+d} - N_b\theta_{1,i-1}\phi_{1,i-1} - N_t\theta_{1,i-1}^2\right] -$$
$$\left.-\frac{1}{6}\left[-\overline{f}_i\overline{\theta}_i - E_c\overline{f}_{2,i}^2 - \frac{n-1}{d}E_c(W_e)^d\overline{f}_{2,i}^{2+d} - N_b\overline{\theta}_{1,i}\overline{\phi}_{1,i} - N_t\overline{\theta}_{1,i}^2\right]\right\} \tag{58}$$

$$\phi_i = \phi_{i-1} + h\left(\frac{2}{3}\phi_{1,i} + \frac{1}{2}\phi_{1,i-1} - \frac{1}{6}\overline{\phi}_{1,i}\right) \tag{59}$$

$$\overline{\phi}_{1,i} = \phi_{1,i-1} + hS_c\left(\frac{2}{3}\left\{-f_i\phi_i - \frac{N_t P_r}{N_b\left(1+\frac{4}{3}R_d\right)}\left[-f_i\theta_{1,i} - E_c f_{2,i}^2 - \frac{n-1}{d}E_c(W_e)^d f_{2,i}^{2+d} - \right.\right.\right.$$
$$\left.-N_b\theta_{1,i}\phi_{1,i} - N_t\theta_{1,i}^2\right] + \gamma\phi_i\Big\} + \frac{1}{2}\left\{-f_{i-1}\phi_{i-1} - \frac{N_t P_r}{N_b\left(1+\frac{4}{3}R_d\right)}\left[-f_{i-1}\theta_{1,i-1} - E_c f_{2,i-1}^2 - \right.\right.$$
$$\left.\left.-\frac{n-1}{d}E_c(W_e)^d f_{2,i-1}^{2+d} - N_b\theta_{1,i-1}\phi_{1,i-1} - N_t\theta_{1,i-1}^2\right] + \gamma\phi_{i-1}\right\} - \frac{1}{6}\left\{-\overline{f}_i\overline{\phi}_i - \frac{N_t P_r}{N_b\left(1+\frac{4}{3}R_d\right)}\cdot\right.$$
$$\left.\left.\left[-\overline{f}_i\overline{\theta}_{1,i} - E_c\overline{f}_{2,i}^2 - \frac{n-1}{d}E_c(W_e)^d\overline{f}_{2,i}^{2+d} - N_b\overline{\theta}_{1,i}\overline{\phi}_{1,i} - N_t\overline{\theta}_{1,i}^2\right] + \gamma\overline{\phi}_i\right\}\right) \tag{60}$$

Results and discussion

The whole domain is divided into some intervals for applying the proposed finite difference scheme. The length of each interval is the same. The numerical scheme is constructed and applied to solve the dimensionless system of boundary values problems (37)-(40). The requirement for applying this scheme is to get first-order differential equations if the equation(s) is not more than first-order. The scheme is employed with the Gauss-Seidel iterative method for the problem considered in this contribution. The iterative method finds the solution of the proposed scheme's difference equation(s). As mentioned, the proposed scheme can only solve first-order differential equations. It can be used to solve high-order linear or non-linear initial value problems. A shooting procedure is utilized to apply this scheme to second or third order boundary value problems. But, the shooting strategy consumes more time to converge. It also requires another scheme for solving equations. In this contribution, Matlab solver solve is considered. Also, the iterative solver requires one initial guess to start the computations. It requires tolerance, so the iterative solver will be stopped when it meets the given criteria, and the final solution can be obtained.

Problem (37)-(40) is also solved with the MATLAB solver bvp4c. This MATLAB solver can solve ODE with boundary conditions. It is high-order accurate and converges fast in most cases. The solver is useful in this study and can be considered a verification tool for checking the accuracy or convergence of the solution obtained by the proposed scheme. The solver requires one initial guess to solve given differential equations. The MATLAB software also contains other solvers to solve differential equations with initial conditions. If the problem is boundary value, then MATLAB solvers can be considered to solve differential equations in a shooting manner.

This contribution employs a numerical scheme for solving second and third-order boundary value problems. A shooting strategy is also employed for this study. Figure 1 shows the absolute error between solutions obtained by the proposed scheme and MATLAB solver bvp4c. The absolute error is computed by finding an absolute difference between two numerical values at each grid point. Figure 2 depicts the effect of the Weissenberg number and magnetic parameter on the velocity profile. From this fig. 2, it can be observed that the velocity profile de-escalates by increasing the Weissenberg number and magnetic parameter. The reason behind this decay due to enhancing magnetic parameters is to accelerate the Lorentz force that resists the particles of the fluid.

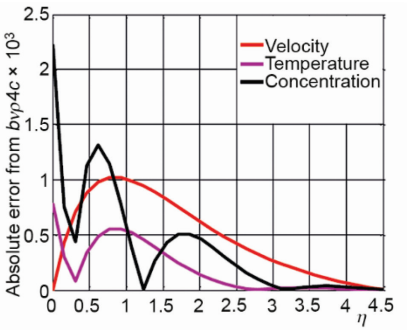

Figure 1. Absolute error of proposed scheme and MATLAB solver bvp4c using $N = 30$, $W_e = 0.1$, $n = 1.5$, $d = 3$, $M = 0.1$, $\beta = 0.1$, $F_r = 0.1$

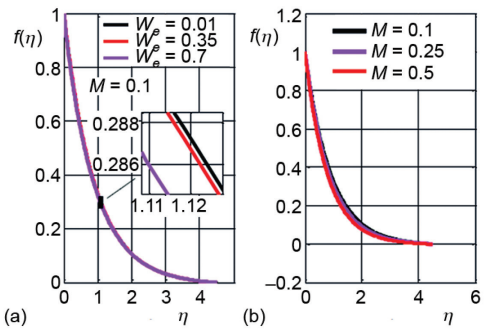

Figure 2. Effect of Weisenberg number and magnetic parameter on velocity profile using $N = 500$, $n = 1.5$, $d = 3$, $\beta = 0.1$, $F_r = 0.1$; (a) $M = 0.1$ and (b) $W_e = 0.1$

Figure 3 deliberates the effect of the inertia coefficient and porosity parameter on the velocity profile. Velocity profile decays by rising values of porosity parameter and inertia coefficient. Since growth in the porosity parameter produces more resistance in the flow and growth in the inertia coefficient enhances the drag force, these factors resist the flow's velocity, leading to decay in the velocity profile. The effect of the thermophoresis parameter and Eckert number on the temperature profile is depicted in fig. 4. Temperature profile decreases by rising values of the thermophoresis parameter and Eckert number. Since thermophoresis force grows by rising thermophoresis parameter, this leads to an increase in the process of transferring fluid particles from the surface of the plate to its surroundings. Shifting particles from one place to another increases the temperature profile. The Eckert number grows in the friction between fluid's particles and raises the temperature profile. The behavior of the temperature profile by variation of radiation parameter and Biot number is portrayed in fig. 5. Temperature profile rises by the increase in radiation parameter and decays by rising Biot number. The rise in temperature profile results from boosting the heat flux due to incoming radiation. The heat flux at the wall increases by growing Biot number,

which results in a rise in temperature at the wall. The concentration profile with the variation of the thermophoresis parameter and Brownian motion parameter is displayed in fig. 6. Concentration profile rises and decays, respectively, by incrementing the thermophoresis parameter and Brownian motion parameter. The influence of the Schmidt number and the reaction rate parameter on the concentration profile is seen in fig. 7. Increases in the Schmidt number and reaction rate parameter lead to a decreasing concentration profile. The decay in the concentration profile due to increasing Schmidt number is the consequence of the de-escalation of mass diffusivity and reduces the concentration profile.

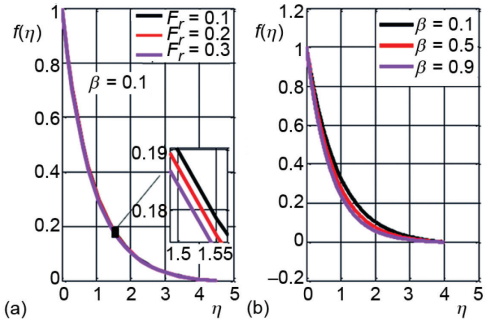

Figure 3. Effect of inertia coefficient and porosity parameter on velocity profile using $N = 500$, $W_e = 0.1$, $n = 1.5$, $d = 3$, $M = 0.1$; (a) $\beta = 0.1$ and (b) $F_r = 0.1$

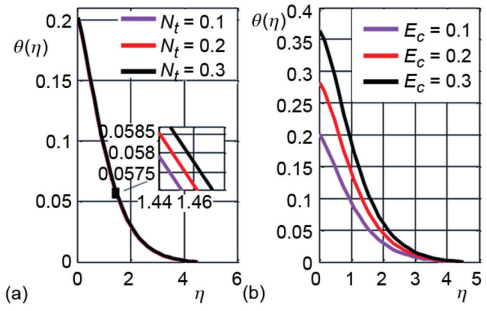

Figure 4. Effect of thermophoresis parameter and Eckert number on temperature profile using $N = 30$, $W_e = 0.1$, $n = 1.5$, $d = 3$, $M = 0.1$, $F_r = 0.1$, $\beta = 0.1$, $N_b = 0.1$, Bi = 0.1, $R_d = 0.1$, $P_r = 1.7$; (a) $E_c = 0.1$ and (b), $N_t = 0.1$

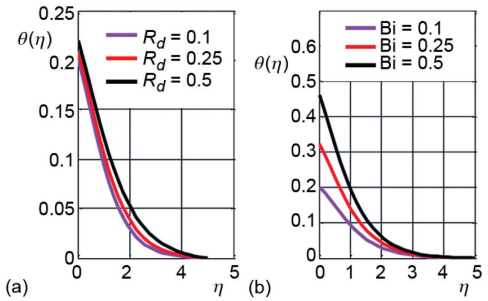

Figure 5. Effect of radiation parameter and Biot number on temperature profile using using $N = 30$, $W_e = 0.1$, $n = 1.5$, $d = 3$, $M = 0.1$, $F_r = 0.1$, $\beta = 0.1$, $N_b = 0.1$, $N_t = 0.1$, $E_c = 0.1$, $P_r = 1.7$; (a) Bi = 0.1 and (b) $R_d = 0.1$

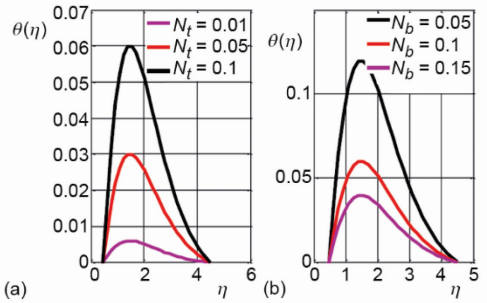

Figure 6. Effect of thermophoresis parameter and Brownian motion parameter on concentration profile using $N = 30$, $W_e = 0.1$, $n = 1.5$, $d = 3$, $M = 0.1$, $F_r = 0.1$, $\beta = 0.1$, $E_c = 0.1$, $S_c = 1.5$, $\gamma = 0.1$; (a) $N_b = 0.1$ and (b) $N_t = 0.1$

Table 1 shows how the proposed method stacks up against some previously published results. This also verifies the solutions obtained by the proposed scheme. Table 2 shows the Weissenberg number, porosity parameter, and inertia coefficient on the skin friction coefficient (excluding the Reynolds number). Skin friction coefficient decays by growing Weissenberg number and porosity parameter values, and it grows by increasing the inertia coefficient. Table 3 shows how the local Nusselt number varies depending on the

Eckert number, the thermophoresis parameter, the Brownian motion parameter, and the radiation parameter (excluding the Reynolds number). For a given set of values, the local Nusselt number increases. Local Sherwood number as a function of thermophoresis, Brownian motion parameter, Schmidt number, and reaction rate parameter are shown in tab. 4 (excluding Reynolds number). Increasing the Brownian motion parameter and decreasing the thermophoresis parameter lead to larger local Sherwood numbers. It does not change (up to four decimal places) by varying the Schmidt number and reaction rate parameter.

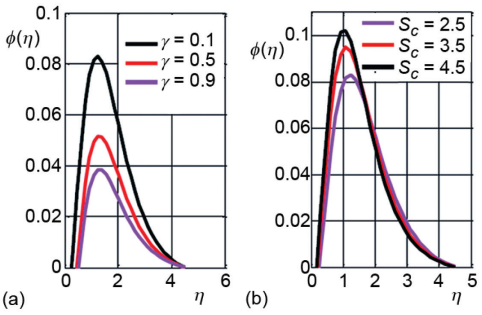

Figure 7. Effect of reaction parameter and Schmidt number on concentration profile using $N = 30$, $W_e = 0.1$, $n = 1.5$, $d = 3$, $M = 0.1$, $F_r = 0.1$, $\beta = 0.1$, $N_b = 0.1$, $N_t = 0.1$; (a) $S_c = 2.5$ and (b) $\gamma = 0.1$(a)

Table 1. Numerical values of $-f''(0)$ using $\beta = 0$ 0 $F_r = W_e = M$

k_p	[29]	[30]	Proposed
0.0	1.000000	1.0000	1.0024
0.5	1.224747	1.2247	1.2251
0.1	1.414217	1.4142	1.4144
1.5	1.581147	1.5811	1.5812
2.0	1.732057	1.7320	1.7321

Table 2 Numerical values of skin friction coefficient (excluding Reynolds number) using $d = 3$, $n = 1.5$, $M = 0.1$

W_e	β	F_r	$R_e^{1/2}C_{fx}$
0.1	0.1	0.1	–1.6847
0.3			–1.7036
0.1	0.3		–1.7800
0.1	0.1	0.3	–1.6667

Table 3. Numerical values for local Nusselt number (excluding Reynolds number) using $d = 3$, $n = 1.5$, $M = 0.1$, $W_e = 0.1$, $\beta = 0.1$, $F_r = 0.1$, $P_r = 1.7$, Bi = 0.1

E_c	N_t	N_b	R_d	$R_e^{1/2}\,\mathrm{Nu}_x$
0.01	0.1	0.01	0.01	0.0602
0.1				0.0813
0.01	0.3			0.0890
	0.1	0.1		0.0891
		0.01	0.1	0.0988

Table 4. Numerical values for local Sherwood number (excluding Reynolds number) using $d = 3$, $n = 1.5$, $M = 0.1$, $W_e = 0.1$, $\beta = 0.1$, $F_r = 0$

N_t	N_b	S_c	γ	$R_e^{1/2}\mathrm{Sh}_x$
0.1	0.1	1.5	0.5	–0.0872
0.3				–0.2614
0.1	0.3			–0.0291
0.1	0.1	2.5		–0.0872
		0.3	0.7	–0.0872

Conclusions

This contribution proposed a numerical scheme for solving linear and non-linear first-order ODE. The scheme required information on the second-order derivative of the dependent variable of given differential equations. The scheme has been employed to solve a dimensionless ODE model of ODE. The model was obtained from a mathematical model of non-Newtonian boundary-layer flow over the flat plate. An iterative scheme was also adopted to solve discretized or difference equations obtained by proposing a scheme on the considered system of ODE. Following this research, different applications for the current approach may be developed. The suggested method may solve various differential equations, including those found in theory and practice. It is relatively easy to implement. Following this research's completion, various applications for the existing method might be developed [31-35]. The concluding thoughts can be stated as

- The velocity profile slightly decayed by incrementing the Weissenberg number.
- Temperature profile escalated by rising Biot number.
- Local Nusselt number escalated by growing radiation parameter.
- The concentration profile was boosted by enhancing the thermophoresis parameter.
- The results are an accurate minimum of two decimal places.

Acknowledgment

The authors wish to express their gratitude to Prince Sultan University for facilitating the publication of this article through the Theoretical and Applied Sciences Lab.

References

[1] Peralta, J. M., *et al.,* Analytical Solutions for the Free-Draining Flow of a Carreau-Yasuda Fluid on a Vertical Plate, *Chem. Eng. Sci., 16831* (2017), Aug., pp. 391-402
[2] Khan, Z., *et al.,* Effect of Thermal Radiation and Chemical Reaction on Non-Newtonian Fluid through a Vertically Stretching Porous Plate with Uniform Suction, *Res. Phys., 9* (2018), June, pp. 1086-1095
[3] Khani, F., *et al.,* Analytical Investigation for Cooling Turbine Disks with a Non-Newtonian Viscoelastic Fluid, *Comput. Mathe. Appl., 61* (2011), 7, pp. 1728-1738
[4] Mahmood, R., *et al.,* A Comprehensive Finite Element Examination of Carreau Yasuda Fluid Model in a Lid Driven Cavity and Channel with Obstacle by Way of Kinetic Energy and Drag and Lift Coefficient Measurements, *J. Mater. Res. Technol., 9* (2020), 2, pp. 1785-1800
[5] Khan, M. I., *et al.,* Theoretical and Numerical Investigation of Carreau-Yasuda Fluid-flow Subject to Soret and Dufour Effects, *Comput. Methods Programs Biomed., 186* (2020), 105145
[6] Kefayati, G. R., Tang, H., Three-Dimensional Lattice Boltzmann Simulation on Thermosolutal Convection and Entropy Generation of Carreau-Yasuda Fluids, *Int. J. Heat Mass Transf., 131* (2019), Mar., pp. 346-364
[7] Khan, M. I., *et al.,* Activation Energy for the Carreau-Yasuda Nanomaterial Flow: Analysis of the Entropy Generation Over a Porous Medium, *J. Mol. Liq., 297* (2020), 111905
[8] Tallmadge, J. A., Gutfinger, C., Entrainment of liquid films. Drainage, withdrawal, and Removal*, Ind. Eng. Chem., 59* (1967), 11, pp. 18-34
[9] Sherwood, J. D., Optimal Shapes for Best Draining, *Phys. Fluids, 21* (2009), 11, 113102
[10] Ungarish, M., Sherwood, J. D., Draining of a thin Film on the Wall of a Conical Container Set into Rapid Rotation about its Vertical Axis*, Phys. Fluids, 24* (2012), 2, 023602
[11] Ali, A., *et al.,* Self-Drainage of Viscous Liquids in Vertical and Inclined Pipes, *Food Bioprod. Process. 99* (2016)*,* July, pp. 38-50
[12] Schunk, P. R., *et al.,* Free-Meniscus Coating Processes, in: *Liquid Film Coating. Scientific Principles and their Technological Implications,* (Kistler, S. F., Schweizer, P. M. Eds.), Springer Netherlands, Dordrecht, 1997, pp. 673-708
[13] Weinstein, S. J., Palmer, H. J., Capillary Hydrodynamics and Interfacial Phenomena, in: *Liquid Film Coating Scientific Principles and Their Technological Implications*, (Kistler, S. F., Schweizer, P. M. Eds.), Springer Netherlands, Dordrecht, 1997, pp. 19-62

[14] Sochi, T., Analytical Solutions for the Flow of Carreau and Cross Fluids in Circular Pipes and Thin Slits, *Rheol. Acta, 54* (2015), 8, pp. 745-756
[15] Eley, R. R., Schwartz, L. W., Interaction of Rheology, Geometry, and Process in Coating Flow*, J. Coat. Technol., 74* (2002), 9, pp. 43-53
[16] Carreau, P. J., Rheological Equations from Molecular Network Theories*, J. Rheol. (Melville, NY, U. S.) 16* (1972), 1, 99
[17] Yasuda, K., Investigation of the Analogies Between Isometric and Linear Viscoelastic Properties of Polystyrene Fluids. Ph. D., Massachusetts Institute of Technology. Dept. of Chemical Engineering., Boston, Mass., USA, 1979
[18] Surana, K. S., *Advanced Mechanics of Continua, Applied and Computational Mechanics Series*, CRC Press, Boca Raton, Fla., USA, 2014
[19] Genovese, D. B., Shear Rheology of Hard-Sphere, Dispersed, and Aggregated Suspensions, and Filler-Matrix Composites*, Adv. Colloid Interface Sci., 171-172* (2012), Mar.-Apr., pp. 1-16
[20] Spikes, H., Jie, Z., History, Origins and Prediction of Elastohydrodynamic Friction, *Tribol. Lett., 56* (2014), 1, pp. 1-25
[21] Brummer, R., *Rheology Essentials of Cosmetic and Food Emulsions*, Springer, Berlin; London, 2006
[22] Hayat, T., *et al.,* Hall and Ohmic Heating Effects On the Peristaltic Transport of Carreau-Yasuda Fluid in an Asymmetric Channel, *Z. Naturforschung, 69* (2014), 1-2, pp. 43-51
[23] Abbasi, F. M., *et al.,* Numerical Analysis for MHD Peristaltic Transportof Carreau-Yasuda Fluid in a Curved Channel with Hall Effects, *J. Magn. Magn. Mater., 382* (2015), May, pp. 104-110
[24] Peralta, J. M., *et al.,* Analytical Solutions for the Free-Draining Flow of a Carreau-Yasuda Fluid on a Vertical Plate, *Chemical Engineering Science, 168* (2017), Aug., pp. 391-402
[25] Rehman, M. I. U., *et al.,* Theoretical Investigation of Darcy-Forchheimer Flow of Bioconvection Casson Fluid in the Presence of Chemical Reaction Effect, On-line first, *Biomass Conv. Bioref.,* https://doi.org/10.1007/s13399-022-03060-5, 2022
[26] Jonnalagadda, J. M., *et al.,* Existence and Stability of Solutions for Nonlinear Impulsive Nabla Fractional Boundary Value Problems of order Less Than One, *Discontinuity, Non-Linearity, and Complexity*, *12* (2023), 2, pp. 231-244
[27] Alzabut, J., *et al.,* Second Order Iterative Dynamic Boundary Value Problems with Mixed Derivative Operators with Applications, *Qual. Theory Dyn. Syst. 22* (2023), Jan., 32
[28] Ijaz Khan, M., *et al.,* Estimation of Entropy Optimization in Darcy Forchheimer flow of Carreau-Yasuda fluid (Non-Newtonian) with First Order Velocity Slip, *Alexandria Engineering Journal, 59* (2020), 5, pp. 3953-3962
[29] Hayat, T., *et al.,* Heat and Mass Transfer for Soret and Dufour's Effect On Mixed Convection Boundary Layer Flow Over a Stretching Vertical Surface in a Porous Medium Filled with a Viscoelastic Fluid, *Commun Non-Linear Sci Numer Simulat, 15* (2010), 5, pp. 1183-1196
[30] Yih, K. A., Free Convection Effect on MHD Coupled Heat and Mass Transfer of a Moving Permeable Vertical Surface, *Int. Commun Heat Mass Transfer, 26* (1999), 1, pp. 95-104
[31] Pasha, S. A., *et al.,* The Modified Homotopy Perturbation Method with an Auxiliary Term for the Non-Linear Oscillator with Discontinuity, *Journal of Low Frequency Noise, Vibration and Active Control, 38* (2019), 3-4, pp. 1363-1373
[32] Arif, M. S., *et al.,* A Stochastic Numerical Analysis for Computer Virus Model with Vertical Transmission Over the Internet, *Computers, Materials & Continua, 61* (2019), 3, pp. 1025-1043
[33] Shatanawi, W., *et al.,* Design of Non-Standard Computational Method for Stochastic Susceptible-Infected-Treated-Recovered Dynamics of Coronavirus Model, *Advances in Difference Equations, 2020* (2020), 505, pp. 1-15
[34] Bibi, M., *et al.,* A Finite Difference Method and Effective Modification of Gradient Descent Optimization Algorithm for MHD Fluid-flow Over a Linearly Stretching Surface*, Computers, Materials & Continua, 62* (2020), 2, pp. 657-677
[35] Nawaz, Y., Arif, M., A New Class of A-Stable Numerical Techniques for Odes: Application to Boundary Layer Flow, *Thermal Science, 25* (2020), 3A, pp. 1665-1675

Paper submitted: December 30, 2022
Paper revised: March 2, 2023
Paper accepted: March 18, 2023